# Simple, stable and efficient nonlinear pulse compression through cascaded filamentation in air

**Tao Pu[1], Kan Tian[1], Bo Hu[1], Zhongjun Wan[1], Linzhen He[1], Xuemei Yang[1], Han Wu[1], Yang Li[1], Weizhe Wang[1,*] and Houkun Liang[1,*]**

[1] *College of Electronics and Information Engineering, Sichuan University, Chengdu 610064, China*

*Correspondence to: H. K. Liang, College of Electronics and Information Engineering, Sichuan University, Chengdu 610064, China. Email: hkliang@scu.edu.cn, W. Z. Wang, College of Electronics and Information Engineering, Sichuan University, Chengdu 610064, China. Email: wangweizhe_1997@163.com.

**Abstract** Nonlinear compression has become an obbligato technique along with the development of ultrafast lasers in generating ultrashort pulses with narrow pulse widths and high peak power. Particularly, techniques of nonlinear compression have experienced a rapid progress as ytterbium (Yb)-doped lasers with pulse widths in the range of hundreds femtoseconds to a few picoseconds stepping into the mainstream laser tools for both scientific and industrial applications. Here, we report a simple and stable nonlinear pulse compression technique with high efficiency through cascaded filamentation in air followed by dispersion compensation. Pulses at a center wavelength of 1040 nm with millijoule pulse energy and 160 fs pulse width from a high-power Yb:$CaAlGdO_4$ regenerative amplifier are compressed to 32 fs, with only 2.4% loss from the filamentation process. The compressed pulse has a stable output power with a root-mean-square variation of 0.2% over one hour time.

*Key words: femtosecond pulse; nonlinear compression; filamentation*

This peer-reviewed article has been accepted for publication but not yet copyedited or typeset, and so may be subject to change during the production process. The article is considered published and may be cited using its DOI.

This is an Open Access article, distributed under the terms of the Creative Commons Attribution licence (https://creativecommons.org/licenses/by/4.0/), which permits unrestricted re-use, distribution, and reproduction in any medium, provided the original work is properly cited.

10.1017/hpl.2023.70

## I. INTRODUCTION

Ultrafast lasers with millijoule pulse energy, tens-watts average power, and a pulse width of few to few-tens fs have found diversified applications such as generations of high-order harmonics [1], intrapulse difference-frequency waves [2], terahertz pulses [3], and isolated attosecond pulses [4]. In the last decade, ytterbium (Yb)-doped lasers have developed rapidly with the superior power scaling capability thanks to the small quantum defects and the availability of high-power laser diodes as the pump source [5], gradually replacing titanium-doped sapphire (Ti:sapphire) lasers which have long been serving as workhorses of scientific ultrafast lasers. Despite of many superior characters, the pulse width of Yb-doped lasers is usually greater than 100 fs [6], limited by the emission bandwidth, which severely hinders the popularization of Yb-doped lasers for the above-mentioned applications.

To further compress the pulse width of Yb-doped lasers, a relatively straightforward strategy is nonlinear pulse compression, with the principle based on the nonlinear spectral broadening and dispersion compensation [7]. A number of techniques have been used for nonlinear spectral broadening of millijoule-level Yb-doped lasers [8-10]. The hollow core fiber (HCF) technique uses hollow waveguides filled with noble gases to extend the nonlinear interaction length between pulses and nonlinear medium, which supports the generation of few-cycle pulses with good beam quality [11]. However, the transmission efficiency of HCF is difficult to exceed 70% [12-14]. Careful alignment and good beam pointing of laser system are also required in HCF compressor. Multiple thin plates using sequences of thin dielectric plates as nonlinear media serve as an effective way for pulse compression with high efficiency [15-17]. However, damages to thin plates and beam quality degradation could be an issue of the laser system stability and long-term operation. Multi-pass cell (MPC) compressors have proven to be able to achieve the extreme



https://doi.org/10.1017/hpl.2023.70 Published online by Cambridge University Press

compression factors with minimum losses, excellent pointing sensitivity, and good beam quality [18,19]. However, traditional MPC modules are based on Herriot cavities which impose relatively complicate beam routings, and require delicate dielectric coatings and gas chambers. Filamentation in gases has been adapted over the past decade to achieve ultrashort pulses. The laser filamentation is sustained when Kerr effect is balanced by the diffraction and plasma defocusing [20], which enables much longer non-diffractive propagation compared to the Rayleigh range with a high intensity. As a result, spectral broadening induced by self-phase modulation (SPM) becomes more prominent. Equipped with a high-pressure gas cell, 0.68 mJ pulses from a Ti:sapphire laser system with a pulse duration of 33 fs were compressed to 5.1 fs, nevertheless, the optical transmission in two cascaded filaments is only 26% owing to the strong ionization loss [21]. In addition, 4 fs pulses were obtained via a single filamentation in a semi-infinite argon gas cell, pumped by 35 fs input pulses, with a low compression efficiency [22]. Besides the large loss, the strong ionization also induces substantial spatial chirp, and confines the good temporal shape only in the beam center. Without the requirement of vacuum apparatuses nor careful control of the gas pressure, pulse compression through filamentation in air has also been demonstrated, generating 22 fs pulses out of 100 fs input pulses. However, the energy coupled into the inner core of the filament which generates the spectral broadening is only 20% of the total input pulse energy, again owing to the strong ionization [23]. In addition, the output stability is another important concern of nonlinear pulse compression. Strong ionization and spectral modulation could induce plasma instability [24,25], which should be avoided in the design of Yb-laser compressors.

In this work, a simple, stable and efficient nonlinear pulse compression technique based on cascaded laser filamentation in air is demonstrated. Pulses with an energy of 1 mJ from Yb-doped laser are compressed from 160 fs to 32 fs with only 2.4% loss from the filamentation process. The



https://doi.org/10.1017/hpl.2023.70 Published online by Cambridge University Press

peak power of the Yb-doped laser system is enhanced from 6.25 GW to 24.7 GW by ~4 times, with good beam quality and spectral homogeneity across the beam profile. The cascaded air filamentation compressor has a superior long-term stability, with the measured power variation < 0.2% over one hour. The demonstrated technique is simple, robust and economical for the efficient pulse compression of Yb-doped lasers, with moderate compression factors (5 times for 2 cascaded compression stages), towards to the acquisition of high peak and average power output.

## II. RESULT

The configuration of the experimental setup is shown in Fig. 1(a). A homemade Yb:$CaAlGdO_4$ (Yb:CALGO) chirped-pulse regenerative amplifier, generating 160 fs pulses, at a central wavelength of 1040 nm and a repetition rate of 20 kHz is used as the experimental platform. In the experiment, 1 mJ pulses with a peak power of 6.25 GW is delivered. The cascaded filamentation compressor consists of two identical modules. Nonlinear spectral broadening is achieved mainly through SPM during the process of laser filamentation in air. Chirped mirrors are placed behind each nonlinear spectral broadening stage to compensate the dispersion. The photos of laser filamentations from the cascaded modules are shown in Fig. 1(b) and (c). The laser before and after nonlinear compression is characterized by an optical spectral analyzer (Yokogawa AQ6370D), a power meter (Ophir FL250A-BB-50), and a beam profiler (Dataray WinCamD). The temporal profiles of the compressed pulses are measured by a commercial second-harmonic generation frequency-resolved optical gating (SHG-FROG) setup (Mesa Photonics).

Prior to the nonlinear compressor, a telescope system is used to adjust the beam size which is crucial for maximizing the spectral broadening, and at the same time minimizing the ionization loss through the process of laser filamentation. After the telescope, p-polarization is adjusted with a half-wave plate to reduce the polarization loss of the chirped mirrors. In the first compression



https://doi.org/10.1017/hpl.2023.70 Published online by Cambridge University Press

stage, pulses with an energy of 1 mJ and a peak power of 6.25 GW which is slightly greater than the critical power of self-focusing in air at a wavelength of 1040 nm are focused in air by using a lens with 500 mm focal length. Loose focusing is desired for a weak ionization and long interaction length. The beam diameter on the lens is ~ 3.5 mm generating a linear peak power density of 18.8 TW/cm2 at the focal spot. As shown in Fig. 1(b), laser filament with a length of ~ 50 mm is formed, through which SPM occurs. The divergent beam is collimated by a lens with a focal length of 750 mm, and the diameter of the collimated beam is made ~ 5 mm.

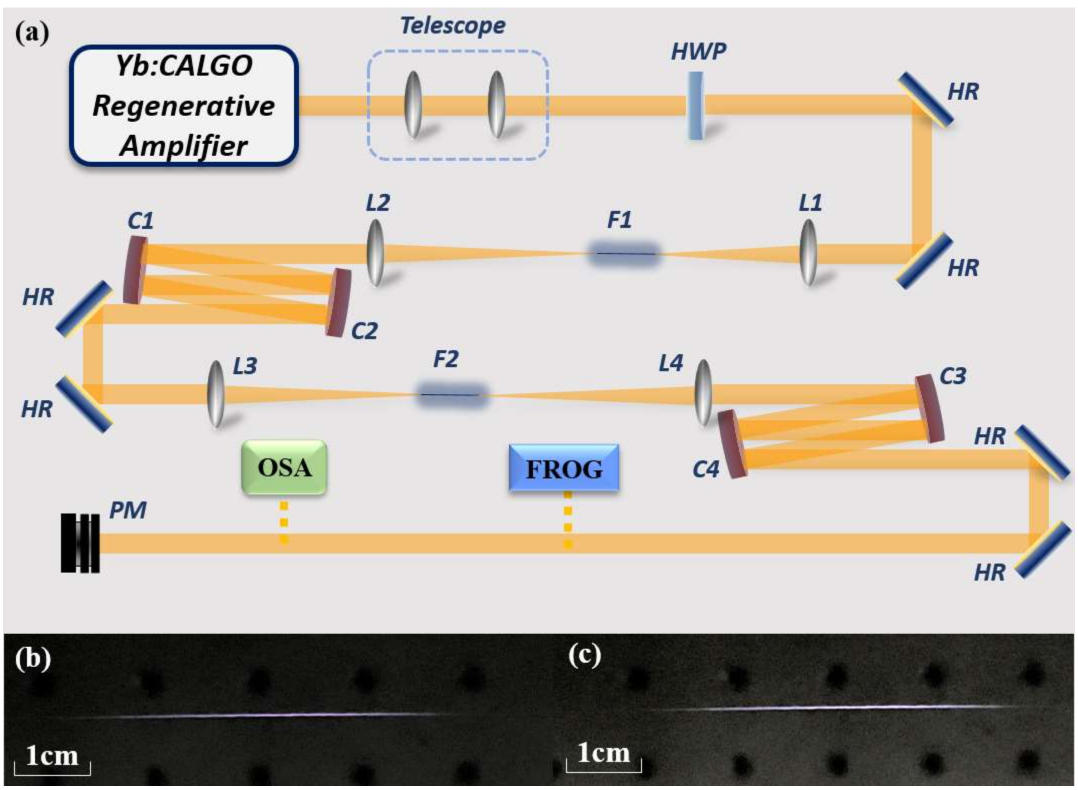


**Fig. 1. (a)** Schematic diagram of the cascaded nonlinear compressor through filamentation in air. HWP, half-wave plate; L, lens; C, chirped mirror; F, filamentation; HR, high reflection mirror; PM, power meter. The photos of the generated filamentation in air in the first **(b)** and second stage **(c)**.

The reason for enlarging the beam size is to avoid damages on subsequent chirped mirrors. After the collimating lens, the beam is reflected 18 times on the chirped mirror pairs, which provide a



https://doi.org/10.1017/hpl.2023.70 Published online by Cambridge University Press

total negative dispersion of -2700 $fs^2$ over the spectral range of 850 -1200 nm. In the second stage, a lens with a focal length of 750 mm is used to focus the beam and a filament in air with a length of 55 mm is generated, as shown in Fig. 1(c). The peak power density is 36.2 $TW/cm^2$. The diverged beam is then collimated by a 750 mm lens and reflected on the chirped mirror pairs for 6 bounces, which supplies a total negative dispersion of -900 $fs^2$.

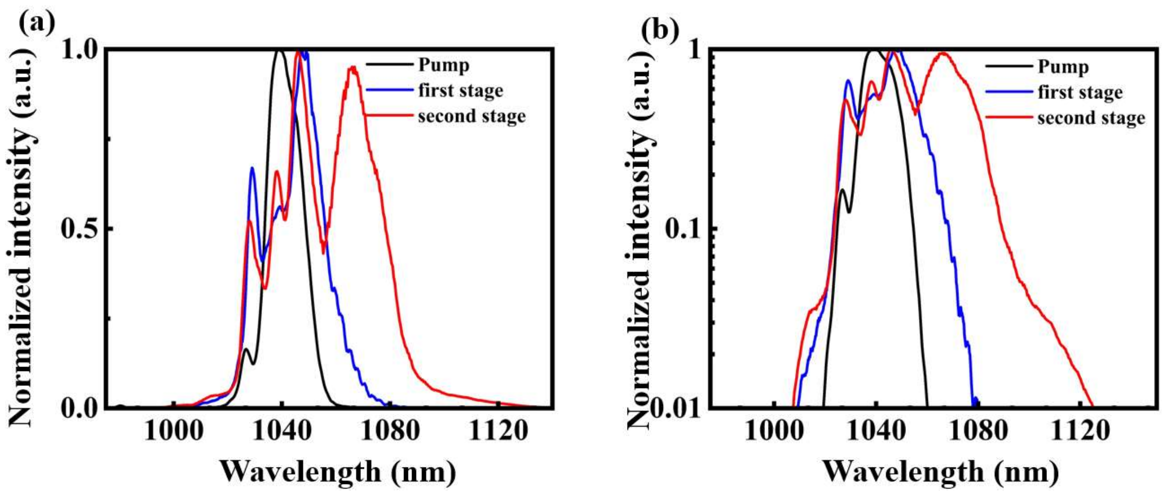


**Fig. 2.** Spectra of the input and the output pulses of each nonlinear compression stage in the linear **(a)** and logarithm **(b)** scales, respectively. Black, blue and red curves are the pump spectra, the spectra after the first and second nonlinear compression stages, respectively.

In Fig. 2, the spectra of the input and the output pulses of the two nonlinear compression stages are compared in both linear and logarithm scales. The black and blue curves present the spectra before and after the first filamentation stage. Spectral broadening spanning from 1010 to 1080 nm at - 20 dB is manifested through the first stage filamentation. The spectrum measured after the second stage filamentation is shown as red curves in Fig. 2, which is significantly broadened compared to blue ones in both linear and logarithm scales, covering a spectral range from 1010 nm to 1130 nm at -20 dB, which supports a transform-limited (TL) pulse width of 30 fs. Notably, in both filamentation stages, red shift is the main force of spectral broadening, which



https://doi.org/10.1017/hpl.2023.70 Published online by Cambridge University Press

indicates that in our experiment the spectral broadening is mainly aroused by the Kerr and Raman effects [26,27] in air, while the plasma generation associated with ionization loss is weak. It is worth mentioning that when the pulse energy varying in the range of 0.8 to 1.5 mJ, similar spectral broadening could be achieved by adjusting the beam size on the focusing lens via the telescope.

The temporal profiles of the pump pulse, the pulse after the first and second nonlinear compression stages are characterized by SHG-FROG as shown in Fig. 3. The measured and retrieved FROG traces of the pump pulse are shown in Fig. 3(a) and (b), respectively. And the pump pulse has a bandwidth of 13 nm, as presented in Fig. 3(c), which supports a TL pulse of 138 fs. The retrieved temporal profile of the pump pulse indicates a pulse width of 160 fs as in Fig. 3(d). The spectral-temporal characteristics of the compressed pulses after the first stage are shown in Fig. 3(e)-(h). The pulse width is compressed from 160 fs to 65 fs, with a TL pulse width of 58 fs, as manifested in Fig. 3(h). The pulse energy after the first nonlinear compression stage is 0.87 mJ, with 85.5% energy contained in the main pulse, generating a peak power of 11.5 GW. In this stage, the losses caused by filamentation and reflections on chirped mirrors are 0.8% and 11.6%, respectively. Fig. 3(i)-(l) characterize the second-stage nonlinear compression. The measured and retrieved spectra have a relatively good agreement as presented in Fig. 3(k). In the second stage, the pulse width is compressed from 65 fs to 32 fs with a pulse energy of 0.83 mJ. 95% of the total energy is contained in the main pulse as presented in Fig. 3(l), which produces a peak power of 24.7 GW. In the second compression stage, losses from laser filamentation and reflections on chirped mirrors are measured as 1.6% and 3%, respectively. After both compression stages the measured and retrieved spectra cannot reproduce the short wavelength sides very well which is mainly due to the slight misalignment during the FROG traces measurement.



https://doi.org/10.1017/hpl.2023.70 Published online by Cambridge University Press

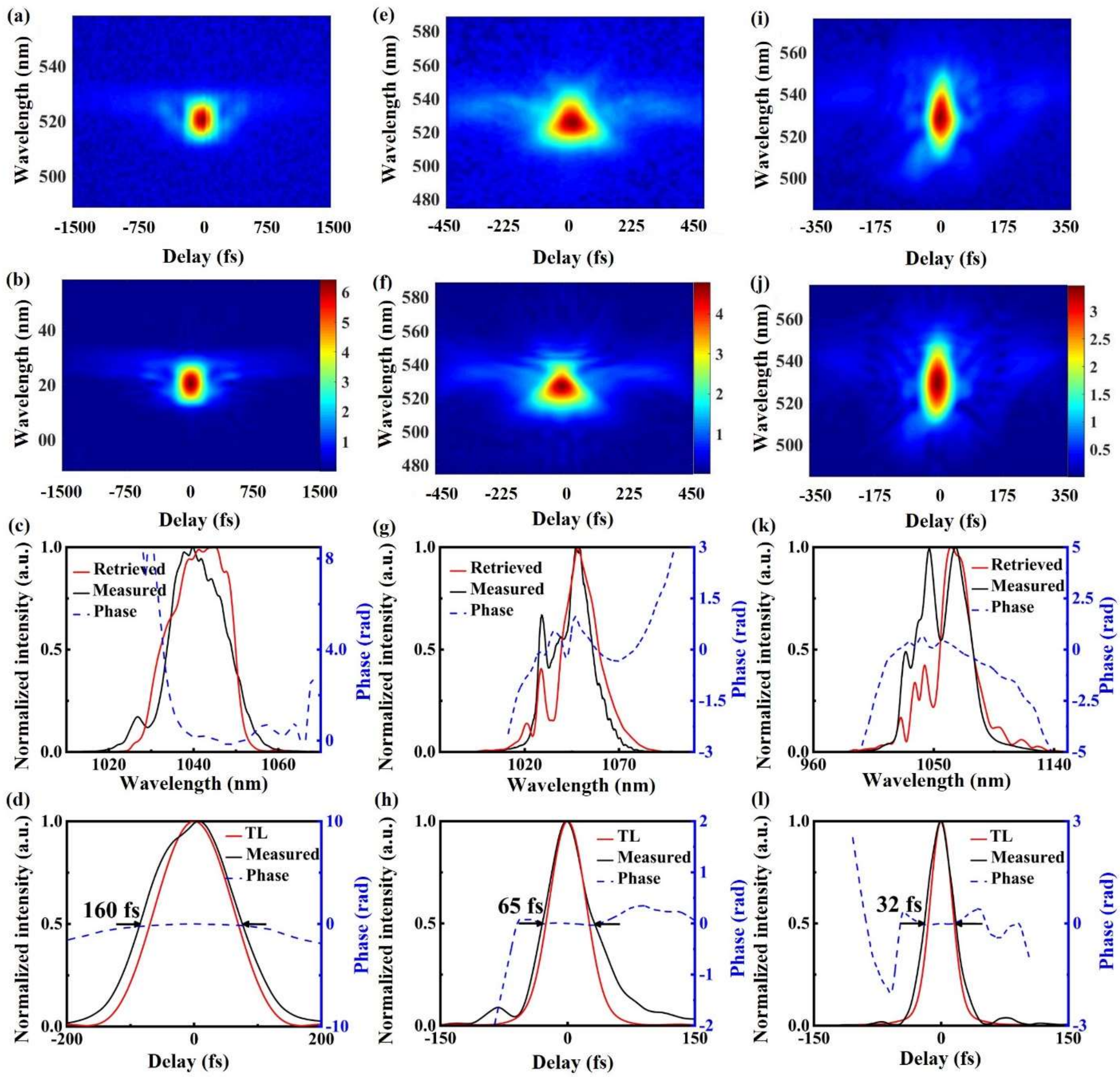


**Fig. 3.** SHG-FROG measurements of the 160, 65, and 32 fs pulses from the Yb:CALGO regenerative amplifier, after the first and second compression stages, respectively. Input pulse: the measured **(a)** and retrieved **(b)** FROG traces. The FROG error is measured as 0.93%. **(c)** The retrieved spectral intensity and phase, compared to the spectrum independently measured using a spectral analyzer. **(d)** The retrieved and TL temporal profiles indicating a measured pulse width of 160 fs. The pulse from the first compression stage: **(e)** and **(f)** are the measured and retrieved FROG traces, respectively. The FROG error is measured as 0.94%. **(g)** The retrieved spectral intensity and phase, compared to the spectrum independently measured using



https://doi.org/10.1017/hpl.2023.70 Published online by Cambridge University Press

a spectral analyzer. **(h)** The retrieved and TL temporal profiles indicating a measured pulse width of 65 fs. The pulse from the second compression stage: **(i)** and **(j)** are the measured and retrieved FROG traces, respectively. The FROG error is measured as 1.09%. **(k)** The retrieved FROG spectral intensity and phase, compared to the spectrum independently measured using a spectral analyzer. **(l)** The retrieved and TL temporal profiles indicating a measured pulse width of 32 fs.

The parameters of the cascaded air filamentation compressor such as the pulse energy, peak power and efficiency are summarized in Table 1. After the cascaded air filamentation compressor, 32 fs pulses with an average power of 16.7 W are obtained and the peak power is increased from 6.25 GW to 24.7 GW. The compression factors of the first and second stage are 2.45 and 2, respectively. Small nonlinear accumulation and weak ionization process in each compression stage avoids the spatio-temporal inhomogeneous of the laser beam. The total efficiency of the nonlinear compressor is 83% while the loss aroused by laser filamentation is only 2.4%, which indicates that the loss is mainly due to the reflection of chirped mirrors. It is worth mentioning that limited by the laboratory space and the availability of chirped mirrors, only two stages of filamentation air compressor are performed in this experiment, but it is foreseeable that by using more stages of air filamentation compressors it’s possible for sub-10 fs pulse generation.

The spatial chirp of the output beam after the cascaded air filamentation nonlinear compressor is also characterized as shown in Fig. 4(a). The spectral shapes remain nearly identical, when scanning the beam across both axes, which indicates there is almost no spatial

**Table 1. Experimental parameters in the two-stage cascaded air filamentation pulse compressor**



https://doi.org/10.1017/hpl.2023.70 Published online by Cambridge University Press

| | *Input energy* | *Output energy* | *Peak power* | *Loss by filamentation* | *Total efficiency* |
|---|---|---|---|---|---|
| *First stage* | *1 mJ* | *0.87 mJ* | *11.5 GW* | *0.8%* | *87.4%* |
| *Second stage* | *0.87 mJ* | *0.83 mJ* | *24.7 GW* | *1.6%* | *95.4%* |

chirp resulted from the cascaded filamentation compressor. The M-square ($M^2$) factor of the output beam after two stages of nonlinear compression is characterized in Fig. 4(b), revealing values of $M^2$ of 1.28 and 1.31 along the x and y axis, respectively. Notably, that the $M^2$ factor of the pump beam is 1.09 and 1.14 along the x and y axis, respectively, which indicates that after nonlinear pulse compression the beam quality is only slightly deteriorated. It is therefore evident that the laser output after the cascaded filamentation in air with weak ionization has a good Gaussian beam profile, negligible spatial chirp, and small temporal pedestals, which indicates a uniform spatial phase resulted from the nonlinear compression process.

To test the stability of the nonlinear compressor the laser system is operated for an hour with an average power of 16.7 W and a pulse energy of 0.83 mJ after nonlinear compression. Fig. 4(c) shows the power stability of the laser output after the cascaded air filamentation compressor. For the measurement time of one hour, the root-mean-square (RMS) power variation of ~ 36,000 consecutive points is ~ 0.2%. The slight decreasing trend in average power is caused by the thermal drift of the Yb:CALGO regenerative amplifier. It is worth noting that the nonlinear compression method proposed here which relies on the cascaded weak ionization could minimize the plasma instabilities in the conventional nonlinear compression techniques, and provide a route towards to a super-stable and super-efficient nonlinear compression process, especially at high repetition rates.



https://doi.org/10.1017/hpl.2023.70 Published online by Cambridge University Press

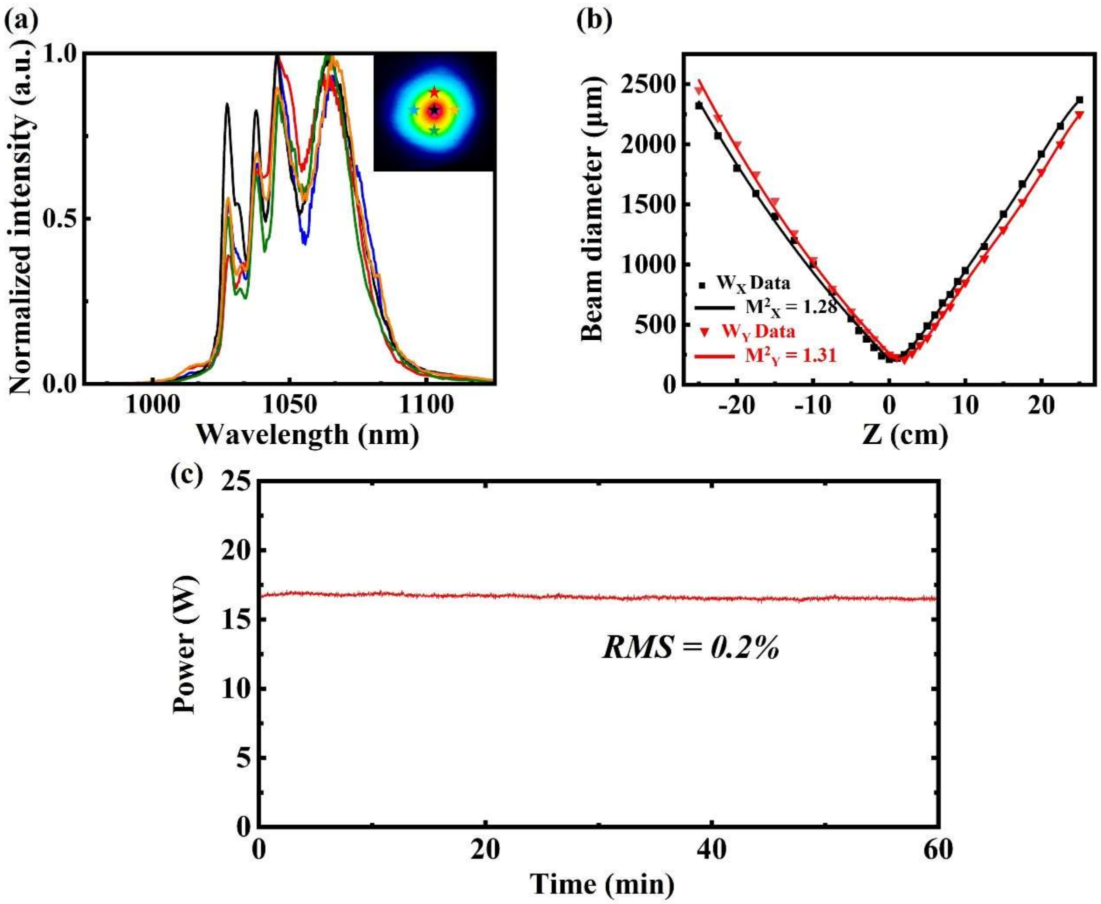


**Fig. 4.** **(a)** The measured spectra at different spatial positions which are indicated by the five stars across the beam as shown in the inset. **(b)** Beam quality measurement after nonlinear compression. **(c)** The measured output power over 1 hour of continuous operation.

## III. CONCLUSION

In conclusion, we demonstrate a simple, stable and efficient nonlinear pulse compression technique by using cascaded laser filamentation in air. The pulse width from a millijoule Yb:CALGO regenerative amplifier is compressed from 160 to 32 fs, with a total transmission efficiency of 83%, in which the loss aroused by filamentation is only 2.4%, and the major loss is from the reflection of chirped mirrors. Thus a peak power of 24.7 GW is achieved. Moreover, the demonstrated technique has a superior stability with a measured output power variation of 0.2%



https://doi.org/10.1017/hpl.2023.70 Published online by Cambridge University Press

over 1 hour. It is worth noting that with more stages of air filamentation compressor, it is possible to obtain sub-10 fs pulses with high efficiency by using customized chirped mirrors. Compared to the MPC, HCF and multi-plate compressors, fine alignment of the pump beam and precise pressure control of gas chambers are not required. In addition, there is no risk of damaging the optical components such as the HCF and thin plates in the nonlinear compressor. Therefore, we believe the developed cascaded air filamentation compressor can provide a new route for generating high energy pulses with a pulse width of 10-30 fs, which can extend the applications of Yb-doped lasers such as high harmonics generation and terahertz rectification.



https://doi.org/10.1017/hpl.2023.70 Published online by Cambridge University Press

# References


1. Popmintchev, T., Chen, M. C., Popmintchev, D., Arpin, P., Brown, S., Ališauskas, S., Andriukaitis, G., Balčiunas, T., Mücke, O. D., Pugzlys, A., Baltuška, A., Shim, B., Schrauth, S. E., Gaeta, A., García, C. H., Plaja, L., Becker, A., Becker, A. J., Murnane, M. M., and Kapteyn, H. C., "Bright Coherent Ultrahigh Harmonics in the keV X-ray Regime from Mid-Infrared Femtosecond Lasers", Science 336, 1287 (2012).
2. Pupeza, I., Sánchez, D., Zhang, J., Lilienfein, N., Seidel, M., Karpowicz, N., Paasch-Colberg, T., Znakovskaya, I., Pescher, M., Schweinberger, W., Pervak, V., Fill, E., Pronin, O., Wei, Z., Krausz, F., Apolonski, A., and Biegert, J., "High-power sub-two-cycle mid-infrared pulses at 100 MHz repetition rate", Nat. Photonics 9, 721 (2015).
3. Zhang, B., Ma, Z., Ma, J., Wu, X., Ouyang, C., Kong, D., Hong, T., Wang, X., Yang, P., Chen, L., Li, Y., and Zhang, J., "1.4-mJ High Energy Terahertz Radiation from Lithium Niobates", Laser Photon. Rev. 15, 2000295 (2021).
4. Gaumnitz, T., Jain, A., Pertot, Y., Huppert, M., Jordan, I., Lamas, F. A., and Wörner, H. J., "Streaking of 43-attosecond soft-X-ray pulses generated by a passively CEP-stable mid-infrared driver", Opt. Express 25, 27506 (2017).
5. Wang, Y., Chi, H., Baumgarten, C., Dehne, K., Meadows, A. R., Davenport, A., Murray, G., Reagan, B. A., Menoni, C. S., and Rocca, J. J., "1.1 J Yb:YAG picosecond laser at 1 kHz repetition rate", Opt. Lett. 45, 6615 (2020).
6. Caracciolo, R., Kemnitzer, M., Guandalini, A., Pirzio, F., Agnesi, A., and Aus der Au, J., "High pulse energy multiwatt Yb:$CaAlGdO_4$ and Yb:$CaF_2$ regenerative amplifiers", Opt. Express 22, 19912 (2014).
7. Nagy, T., Simon, P., and Veisz, L., "High-energy few-cycle pulses: post-compression techniques", Adv. Phys.: X 6, 1845795 (2021).
8. Piccoli, R., Rovere, A., Jeong, Y. G., Jia, Y., Zanotto, L., Légaré, F., Schmidt, B. E., Morandotti, R., and Razzari, L., "Extremely broadband terahertz generation via pulse compression of an Ytterbium laser amplifier", Opt. Express 27, 32659 (2019).
9. Lu, C. H., Wu, W. H., Kuo, S. H., Guo, J. Y., Chen, M. C., Yang, S. D., and Kung, A. H., "Greater than 50 times compression of 1030 nm Yb:KGW laser pulses to single-cycle duration", Opt. Express 27, 15638 (2019).




https://doi.org/10.1017/hpl.2023.70 Published online by Cambridge University Press

10. Kaumanns, M., Pervak, V., Kormin, D., Leshchenko, V., Kessel, A., Ueffing, M., Chen, M., and Nubbemeyer, T., "Multipass spectral broadening of 18 mJ pulses compressible from 1.3 ps to 41 fs", Opt. Lett. 43, 5877 (2018).
11. Ouillé, M., Vernier, A., Böhle, F., Bocoum, F. M., Jullien, A., Lozano, M., Rousseau, J. P., Cheng, Z., Gustas, D., Blumenstein, A., Simon, P., Haessler, S., Faure, J., Nagy, T., and Lopez-Martens, R., "Relativistic-intensity near-single-cycle light waveforms at kHz repetition rate" Light Sci. Appl. 9, 47 (2020).
12. Haddad, E., Safaei, R., Leblanc, A., Piccoli, R., Jeong, Y. G., Ibrahim, H., Schmidt, B. E., Morandotti, R., Razzari, L., Légaré, F., and Lassonde, P., "Molecular gases for pulse compression in hollow core fibers", Opt. Express 26, 25426 (2018).
13. Nagy, T., Hädrich, S., Simon, P., Blumenstein, A., Walther, N., Klas, R., Buldt, J., Stark, H., Breitkopf, S., Jójárt, P., Seres, I., Várallyay, Z., Eidam, T., and Limpert, J., "Generation of three-cycle multi-millijoule laser pulses at 318 W average power", Optica 6, 1423 (2019).
14. Klas, R., Eschen, W., Kirsche, A., Rothhardt, J., and Limpert, J., "Generation of coherent broadband high photon flux continua in the XUV with a sub-two-cycle fiber laser", Opt. Express 28, 6188 (2020).
15. Guo, J., Gao, Z., Sun, D., Du, X., Gao, Y., and Liang, X., "An efficient high-power femtosecond laser based on periodic-layered-Kerr media nonlinear compression and a Yb:YAG regenerative amplifier", High Power Laser Sci. Eng. 10, 10 (2021).
16. Wang, W. Z., Pu, T., Wu, H., Li, Y., Wang, R., Sun, B., and Liang H. K., "High-power Yb:CALGO regenerative amplifier and 30 fs output via multi-plate compression", Opt. Express 30, 22153 (2022).
17. Zhang, S., Fu, Z., Zhu, B., Fan, G., Chen, Y., Wang, S., Liu, Y., Baltuska, A., Jin, C., Tian, C., and Tao, Z., "Solitary beam propagation in periodic layered Kerr media enables high-efficiency pulse compression and mode self-cleaning", Light: Sci. Appl. 10, 53 (2021).
18. Balla, P., Wahid, A. B., Sytcevich, I., Chen, G., Viotti, A. L., Silletti, L., Cartella, A., Alisauskas, S., Tavakol, H., Uwe, G. W., Schönberg, A., Seidel, M., Trabattoni, A., Manschwetus, B., Tino, L., Calegari, F., Couairon, A., L'Huillier, A., Arnold, C. L., Hartl, I., and Heyl, C. M., "Postcompression of picosecond pulses into the few-cycle regime", Opt. Lett. 45, 2572 (2020).



https://doi.org/10.1017/hpl.2023.70 Published online by Cambridge University Press

19. Hanna, M., Guichard, F., Daher, N., Bournet, Q., Délen, X., and Georges P., “Nonlinear Optics in Multipass Cells”, Laser&Photonics Reviews. 15, 2100220 (2021).
20. Couairon, A., and Mysyrowicz, A., "Femtosecond filamentation in transparent media", Phys. Reports 441, 47 (2007).
21. Hauri, C. P., Guandalini, A., Eckle, P., Kornelis, W., Biegert, J., and Keller, U., "Generation of intense few-cycle laser pulses through filamentation – parameter dependence", Opt. Express 13, 7541 (2005).
22. Steingrube, D. S., Kretschmar, M., Hoff, D., Schulz, E., Binhammer, T., Hansinger, P., Paulus, G. G., Morgner, U., and Kovacev, M., "Sub-1.5-cycle pulses from a single filament", Opt. Express 20, 24049 (2012).
23. Varela, O., Alonso, B., Sola, I. J., Román, J. S., Zaïr, A., Méndez, C., and Roso, L., "Self-compression controlled by the chirp of the input pulse", Opt. Lett. 35, 3649 (2010).
24. Kato, Y., Mima, K., Miyanaga, N., Arinaga, S., Kitagawa, Y., Nakatsuka, and M., Yamanaka, C., "Random Phasing of High-Power Lasers for Uniform Target Acceleration and Plasma-Instability Suppression", Phys. Rev. Lett. 53, 1057 (1984).
25. Epperlein, E., M., "Kinetic theory of laser filamentation in plasmas", Phys. Rev. Lett. 65, 2145 (1990).
26. Carlo, V., Mostafa, S., Aleksandr, K., Leonid, L., and Christoph, P. H., "High-power femtosecond Raman frequency shifter", Opt. Lett. 41, 4719 (2016).
27. Carpeggiani, P. A., Coccia, G., Fan, G., Kaksis, E., Pugžlys, A., Baltuška, A., Piccoli, R., Jeong, Y.-G., Rovere, A., Morandotti, R., Razzari, L., Schmidt, B. E., Voronin, A. A., and Zheltikov, A. M., "Extreme Raman red shift: ultrafast multimode nonlinear space-time dynamics, pulse compression, and broadly tunable frequency conversion", Optica 7, 1349 (2020).




https://doi.org/10.1017/hpl.2023.70 Published online by Cambridge University Press